14TH CANADIAN MASONRY SYMPOSIUM
MONTREAL, CANADA
MAY 16TH – MAY 20TH, 2021

MODELLING OF SHEAR CRITICAL REINFORCED CONCRETE INFILLED FRAMES

Brodsky, Alex[1] and Bentz, Evan[2]

ABSTRACT

Reinforced Concrete (RC) infilled frame structures are widely used for public and residential buildings. When a RC frame with inadequate reinforcement details is subjected to extreme loads, shear failure of the frame may occur. This brittle failure mode is unwanted, and different efforts are invested in preventing this failure mode, e.g., strengthening the RC frame. To examine the behaviour of RC infilled frames under such extreme loads and evaluating its shear capacity, the model required to be able to represent the non-linear response of RC. This includes the post cracking tension stiffening, compression softening due to transverse cracking, shear slip along crack surfaces, reinforcement yielding and strain hardening, etc. The present paper presents a detailed two-dimensional model of the RC frame and employed the constitutive relations of the Modified Compression Field Theory (MCFT), which is found to be a good predictor of RC members and in particular the shear behaviour. The infill wall is replaced by multiple struts, which allow representing the infill-frame interaction. The effect of reinforcement details (longitudinal and transverse), the cross-sectional area of the RC frame, and the infill-wall contact length on the infilled frame response and the failure mode are examined.

KEYWORDS: *infill walls, infilled frames, MCFT, reinforced concrete, shear failure*

[1] Postdoctoral fellow, Department of Civil and Mineral Engineering, University of Toronto, 35 St. George Street, Toronto, ON M5S1A4, Canada. Email: alex.brodsky@utoronto.ca

[2] Professor, Department of Civil and Mineral Engineering, University of Toronto, 35 St. George Street, Toronto, ON M5S1A4, Canada. Email: bentz@civ.utoronto.ca

INTRODUCTION

The combination of a relatively strong infill and weak frame or a frame with poor reinforcement details may lead to a failure of the frame elements during a strong earthquake. When the infill wall is built partially to a certain height of the column it leads to even a more severe condition, known as a short-column effect. In this case, the RC column usually fails in shear. Shear failure of the RC frame was observed in different earthquakes, as documented in Nicola et al. [1], Alih and Vafaei [2], and in laboratory tests, e.g., Mehrabi et al. [3], Colangelo [4], Gao et al. [5] and Basha and Kaushik [6].

During extreme events, such as earthquakes and supporting column failure, the structure undergoes large deformations. At these deformations, the infill wall starts interacting with the surrounding RC frame. This interaction increases the flexural and shear demands of the RC frame's elements. If the frame was not designed to overcome the additional demands as a result of the interaction with the infill wall, it may fail.

While the one-dimensional fiber models of the frame may adequately represent the flexural behaviour of the frame, the behaviour and the deformation of the joint regions and shear failure and deformation are much harder to be represented using these simplified elements. While the response of a bare frame can be easily represented using an adequate fiber-based model, the complex two-dimensional stress state at the infill-frame interaction regions requires a more sophisticated modelling strategy.

The goal of the present study is to investigate the response of shear-critical RC infilled frames using a tool that allows capturing the complex non-linear response of the RC frame in particular at the infill-frame interaction regions.

A TWO-SCALE MODELLING TECHNIQUE

To overcome the limitations of the fiber-based element to represent the complex two-dimensional stress state at the interaction regions, the frame is modelled in detail by two-dimensional elements and the constitutive relations of the Modified Compression Field Theory [7] are applied. Thus, the two-dimensional stress state of the RC elements is explicitly considered. Additionally, the non-linear response of the frame, such as cracking, crushing, tension stiffening and softening of the concrete, and yielding and rapture of the reinforcement is also taken into account.

While the RC frame is modelled by two-dimensional elements, the infill wall is replaced by a struts model. Thus, the presented modelling techniques combines two detailing levels: a macro level for the infill wall and a micro-level for the RC frame. Generally, even the most detailed micro models of the infill wall have difficulties in the prediction of the infill wall's pattern of cracking. Thus, the infill wall modelled by a simplified model , while the frame modelled in detail.

This is not surprising since even when testing two similar walls, made of similar masonry units, built with the same mortar mixture and loaded under similar conditions, typically the two walls

will not have identical cracking patterns as a result of the different imperfections of the mortar joints in each wall.

The inability of the detailed micro models to predict the infill cracking impairs the ability of the models to evaluate the infill-frame interaction since infill cracks directly affect the contact regions and the interfacial stresses along these regions. Consequently, the added complexity and effort does not typically result in a proportionate improvement to accuracy. Therefore, to reduce the computational time, the infill wall is replaced by three struts in each loading direction. The two off-diagonal struts tend to represent the increase of the flexural and shear demand in the frame elements. The struts are parallel, which dictates that the ratio between the beam contact length and its span (α_b) is equal to the ratio between the column contact length and its height ($\alpha_c = \alpha$). Even more importantly, this assumption dictates a similar constitutive relation for all the struts, as presented below.

NUMERICAL MODEL

The behaviour of a single bay infilled frame subjected to monotonic lateral load is investigated here. The geometry and the boundary conditions are illustrated in Figure 1. The base beam is modeled by a steel material with similar equivalent flexural stiffness as the upper beam to decrease the number of elements along this beam.

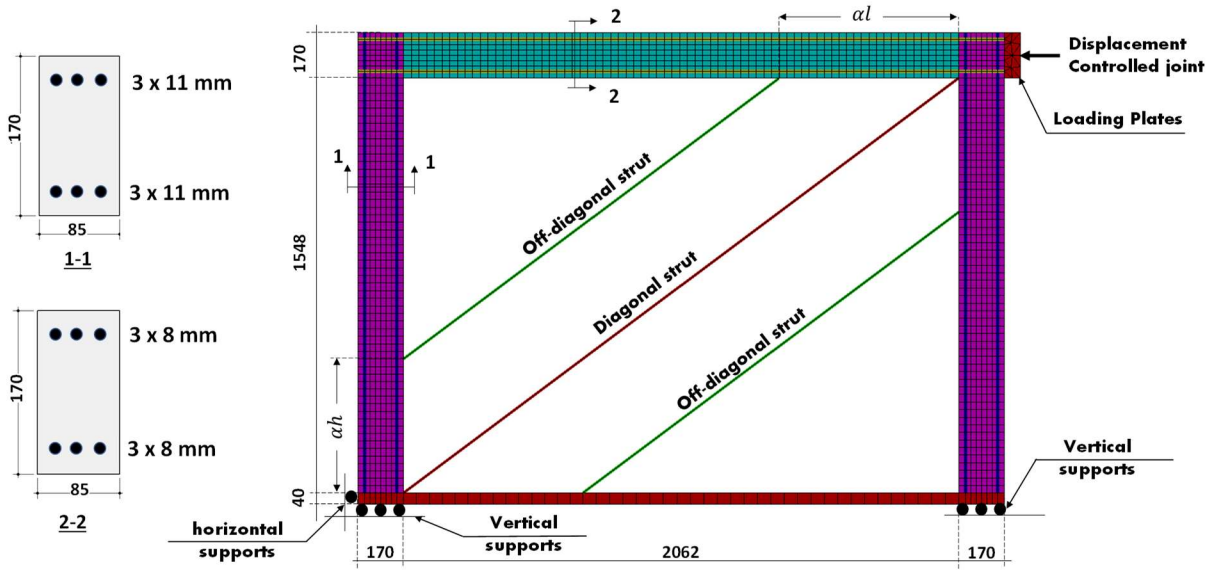

Figure 1: Infilled frame numerical model

MATERIAL MODELS

Concrete material

The Hognestad [8] parabola represent the compressive behaviour of the concrete up to the peak. This relation is suitable for concrete strengths up to about 40 MPa. The stress-strain curve is described according to the following relationship:

$$f_c = -f_c^{'}\left\{2\left(\frac{\varepsilon_c}{\varepsilon_0}\right)-\left(\frac{\varepsilon_c}{\varepsilon_0}\right)^2\right\}, \qquad \varepsilon_c < 0 \tag{1}$$

Where f'_c is the concrete cylindrical compressive strength and ε_0 is the strain at the peak. A linear descending branch represents the response after the peak according to Park, Priestly and Gill [9]. Before cracking, the concrete behaves linear-elastically in tension as follows:

$$f_c = E_c\varepsilon_c, \qquad 0 < \varepsilon_c < \varepsilon_{cr} \tag{2}$$

Where ε_{cr} is the cracking strain and E_c is the initial tangent elastic modulus. The cracking strain is the strain where the concrete reach its tensile strength (f'_t).

$$f_t^{'} = 0.33\sqrt{f_c^{'}} \tag{3}$$

After the cracking, the tensile strength is not dropping to zero thanks to the concrete between the cracks. The tensile stress decays as the tensile strain increases according to the tension stiffening relationship proposed by Bentz [10]. The values of all the mentioned above parameters are listed in Table 1.

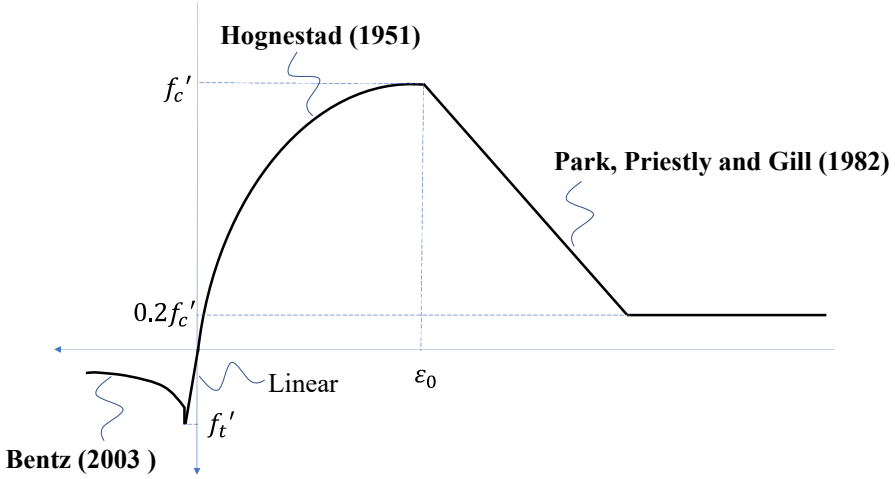

Figure 2: Concrete stress-strain relationship

Reinforcement

The stress-strain relationship of the reinforcement is composed of three linear parts as illustrated in Figure 3. The response includes a linear-elastic response up to yielding, then plateau and strain hardening linear response up to the rapture of the reinforcement. The longitudinal bars are modelled as discrete reinforcement using two-node truss elements while the transverse reinforcement is modelled as smeared over the entire element. The values of the parameters that define the relationship are listed in Table 1.

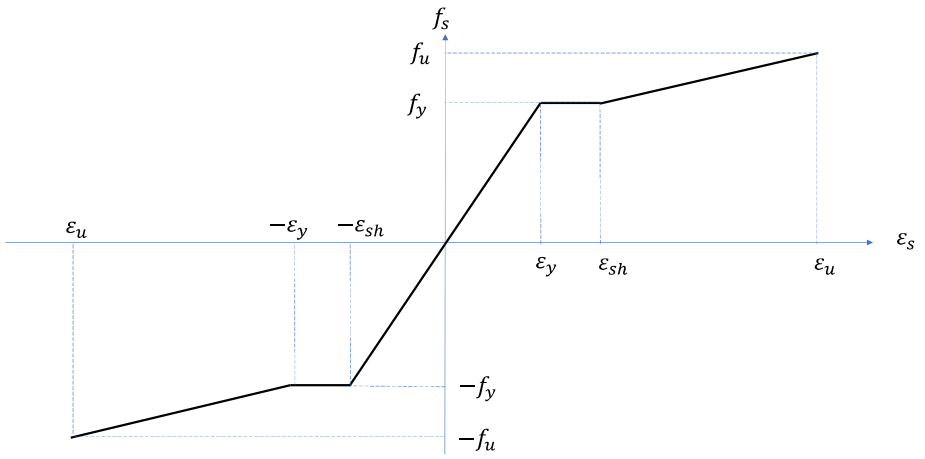

Figure 3: Reinforcement stress-strain relationship

Table 1: Concrete and reinforcement properties

		Parameter	**Value**
Concrete	$f_c^{'}$	Cylinder compressive strength [MPa]	30
	$f_t^{'}$	Tensile strength [MPa]	1.81
	ν	Poisson's ratio	0.15
	E_c	Initial tangent elastic modulus [GPa]	27.39
Reinforcement	ρ_v	Ratio of transverse reinforcement [%]	0.2
	f_y	Yield strength [MPa]	400
	f_u	Ultimate strength [MPa]	600
	E_s	Elastic modulus [GPa]	200
	ε_{sh}	Strain at the onset of strain hardening [mm/m]	10
	ε_u	Strain at the ultimate strength [mm/m]	150

Infill wall

The properties of the struts that replaced the infill wall are determined according to the procedure proposed and validated by Brodsky [11]. The struts properties are determined based on the response of the infill wall in a rigid steel pinned frame. The frame itself is a mechanism and the resistance to external load is attributed to the infill wall and its interaction with the frame. Moreover, increasing the cross-sectional area of the stiff frame has a negligible effect on the response. Thus, the load–displacement curve of the test is used to define the simplified struts model of the infill. The validation of this method against experimental data on large scale RC infilled frames is described in Brodsky [11].

The properties of the struts in the present paper are based on the tests performed by Markulak et al. [12]. Two similar infill walls made of perforated clay units (190x120x90 mm^2) tested in a

pinned rigid frame up to their maximal resistance. The post-peak softening was not examined. For the present study, the response of the infill up to the peak is enough since typically the infill does not reach its ultimate capacity when a shear failure of the RC element occurs. The response of the infill up to the maximal resistance is represented by a bi-linear curve. It is important to note that the Two-scale modelling technique presented here is general and every other strut/s model can be implemented similarly.

The parameters that define the constitutive relation of the struts are listed in Table 2, where A_D and A_{OD} are the cross-sectional area of the diagonal and the off-diagonal struts, ε_y and ε_u are the yielding and the ultimate (rapture) strains, and f_y and f_u are the respective stresses. The modulus of elasticity of the struts is equals to the modulus of elasticity of the masonry infill, 4014 MPa. Three different locations of the off-diagonal struts are examined: α equals 0.16 that represents a short infill-column contact region of 250 mm, and α equals 0.48 that represents 750 mm of the infill-column contact region.

Table 2: Struts' properties

α	A_D	A_{OD}	ε_y	ε_u	f_y	f_u
	[mm^2]	[mm^2]	[mm/m]	[mm/m]	[MPa]	[MPa]
0.16	2022	848	-4.34	-15.51	-17.43	-19.97
0.48	2721	701	-4.34	-15.51	-17.43	-19.97

PARAMETRIC STUDY

Five models (M1 to M5) with different properties are under investigation in the current study. The properties of each model are listed in Table 3. Model M1 is a bare frame model and models M2 and M3 include the same frame with the struts. In each model, the off-diagonal struts connected in different locations as listed in the table. Model M4 used to examine the effect of the thickness of the frame (i.e., frames element's cross-sectional area). The geometry of model M5 is the same as models M1-M3, but it includes a reduction of the reinforcement ratios. The transverse reinforcement ratio is 0.1% and the longitudinal reinforcement consists of four 10 mm bars in the column and four 8 mm bars in the beams (two on each side).

RESULTS

A two-dimensional non-linear FEA is performed using VecTor2 program [13]. This program uses a smeared, rotating-crack formulation for RC based on the Modified Compression Field Theory (MCFT) [7]. The have been extensively validated through experimental tests [13] and effects such as shear slip along crack surfaces, tension stiffening, compression softening due to transverse cracking, and shear deformation can be systematically considered.

Table 3 : Models' parameters

Model	α Parameter [-]	Frame thickness [mm]	Reinforcement	Stiffness [kN/mm]	Capacity [kN]
M1	Bare	85	Original	1.46	31.5
M2	0.16	85	Original	5.04	91.3
M3	0.48	85	Original	4.74	88.1
M4	0.16	340	Same rein. ratio	9.45	179.0
M5	0.16	85	Reduced	4.54	75.9

A displacement-controlled analysis was carried out with a step size of 1.0 mm. A convergence ratio limit of 1.00001 on the calculated displacements were chosen for all the analyses. Models M2-M5 include 1910 nodes and 2103 elements (20 triangular, 1650 rectangular and 433 truss elements). The triangular element is a three-noded element with a total of six degrees of freedom and constant strains and stresses throughout the element. The rectangular element is a four-noded plane stress element with linear gradients of strains and stresses across its width and height.

In the following the effect of the infill wall, different contact regions (locations of the off-diagonal struts), frame's thickness and reinforcement details on the global and local responses of the infilled frames is investigated.

Infill and contact region

The load-displacement curve of models M1, M2 and M3 is presented in Figure 4. The resistance of the infilled frames is about three times higher than the resistance of the same bare frame. As expected, the different locations of the off-diagonal struts have no effect on the initial stiffness. In this case the different location has only a minor effect on the global behavior in the non-linear region. The difference between the resistances is less than 4%. The bare frame failed in a flexural mode with four plastic hinges at the beam-column joints.

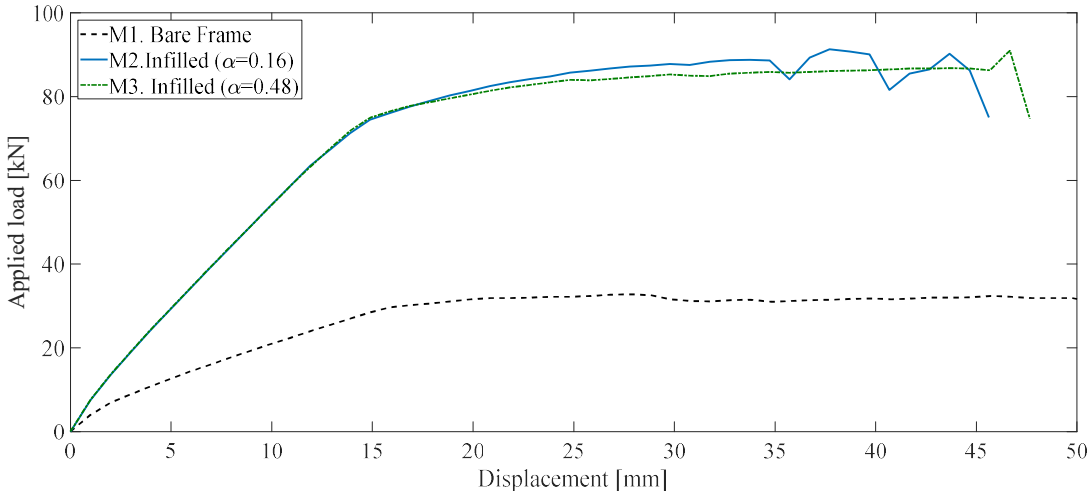

Figure 4: Load-displacement curves of frames with thickness of 85 mm

While the global response is similar, the failure mode of the two infilled frames is different. To examine the failure mode of the model with the short contact region (M2), Figure 5 shows the percentage of a crushing failure of the concrete within each element. In this figure, the average principal compressive stress (f_{c2}) in the concrete is divided by the crushing strength of the concrete (known as f_{c2max} in the Modified Compression Field Theory) given the extent of tensile straining and cracking within that element. As can be seen, the percentage of crushing has locally reached 100% and is predicted to occur almost all over the column width. This indicates a shear failure of the column while the struts are still active, i.e. bellow their ultimate strain.

Figure 6 shows the same distribution in model M3. In this case there is no evidence of crushing of the compressive struts. In this case the off-diagonal struts located far away from the beam-column joint. Consequently, the flexural demands are increased and the longitudinal reinforcement at the column base yields. Thus, cracks with significant width develop at these regions.

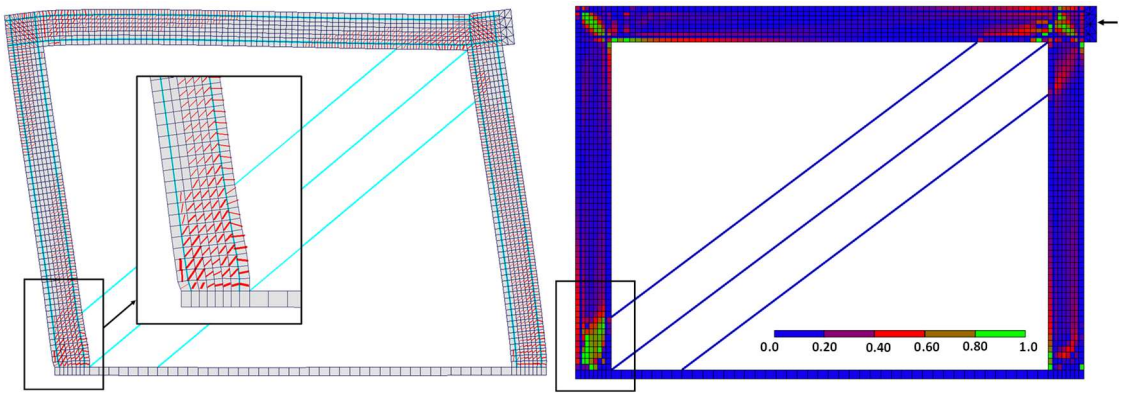

Figure 5: Model M2: pattern of cracking (left) and percentage of a crushing failure of the concrete (right)

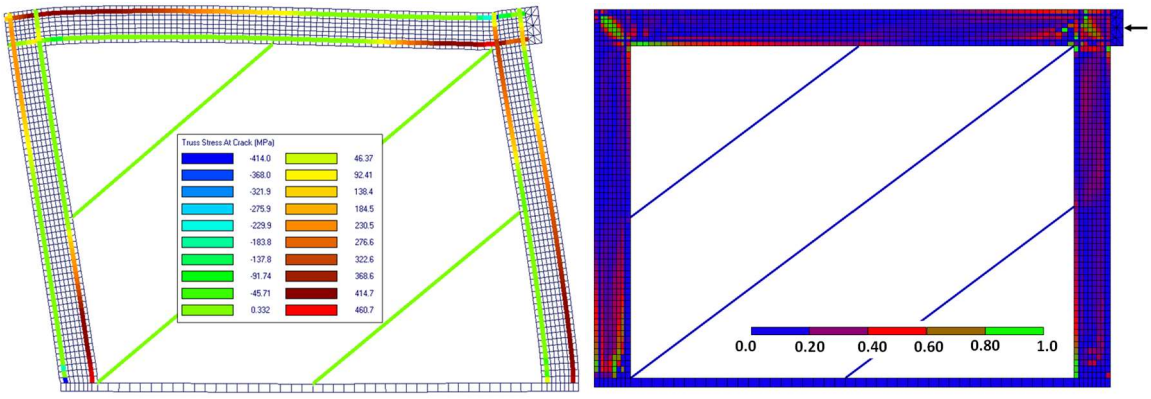

Figure 6: Model M3: stress in the longitudinal reinforcement (left) and percentage of a crushing failure of the concrete (right)

Frame's thickness

One way to prevent the shear failure observed in model M2 is to increase the cross-sectional area of the columns. The thickness of the frame in model M4 is four times higher than the original frame while keeping the reinforcement ratios similar to models M1-M3. Figure 7 presents the response of the bare frame and the two models with the short contact region (α = 0.16). As expected, the increase of the cross-sectional area leads to increase of the initial stiffness and the capacity. While model M2 failed in shear, model M4 reaches the ultimate capacity of the struts. After the contribution of the struts drop to zero, the frame fails in a flexural mode similar to a bare frame.

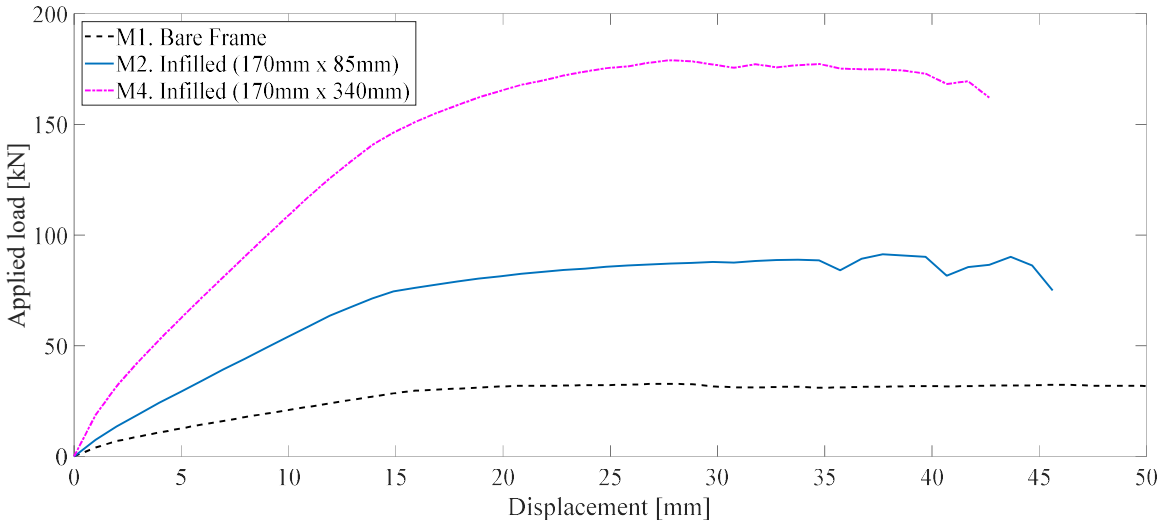

Figure 7: Load-displacement curves of frames with struts that connected at $\alpha = 0.16$

Reinforcement

Model M2 failed because of crushing of the concrete. Model M5 tends to examine a similar frame but with reduced amount of reinforcement. The transverse reinforcement reduced by half to 0.1% and the longitudinal reinforcement of model M5 consists of four 10 mm bars in the column and four 8 mm bars in the beams (two on each side). As expected, the initial stiffness is independent of the amount of reinforcement and the capacity of model M5 decreases (-17%).

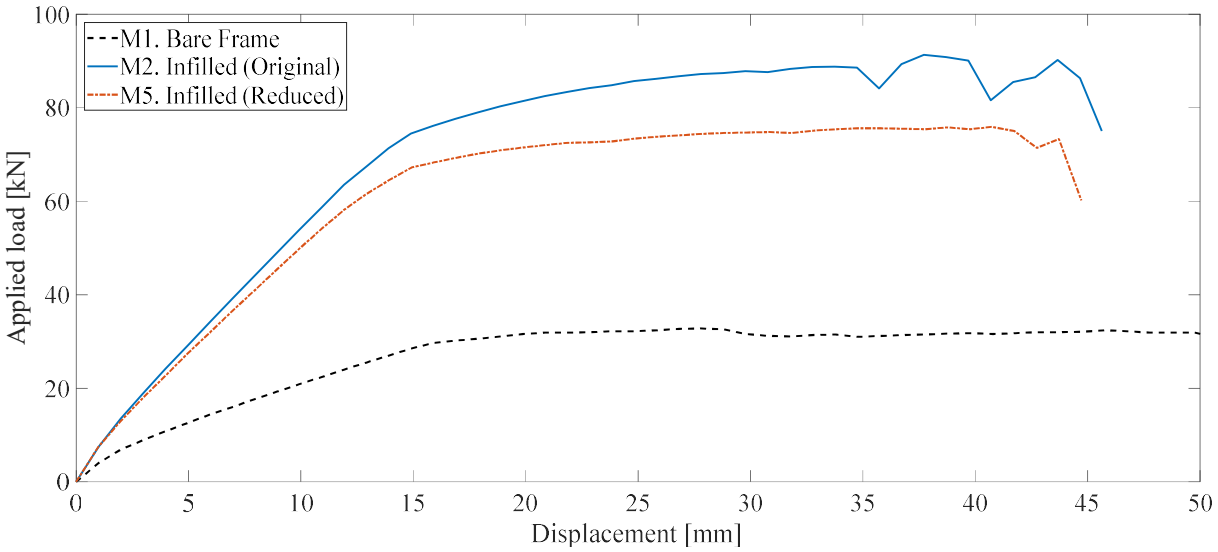

Figure 8: Reinforcement details

The decrease of the amount of the reinforcement effect also the failure mode of the infilled frame. The concrete in model M5 is not crushed but yielding of the longitudinal and transverse reinforcement is observed at the bottom of the columns (Figure 9).

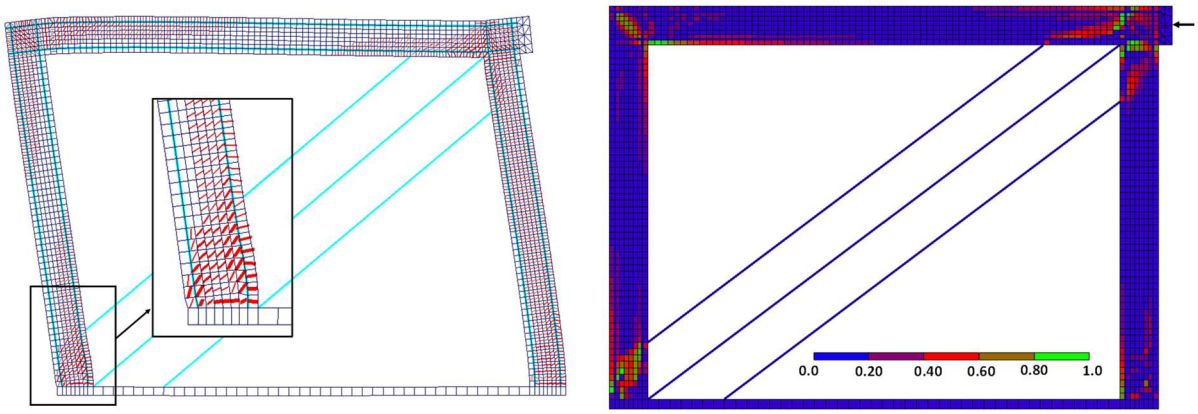

Figure 9: Model M5: stress in the longitudinal reinforcement (left) and percentage of a crushing failure of the concrete (right)

SUMMARY

The effect of the infilled frame properties on its response have been investigated using a two-scale modelling technique. The study showed that the two-scale combination allows investigating the behaviour of infilled frame, capture its non-liner response, and examine the failure mode of the RC frame. The parametric study showed the effect of different infill-frame contact regions, frame's cross-sectional area and reinforcement details on the failure mode of the frame.

ACKNOWLEDGEMENTS

Financial support for this study has been provided by the Lyon Sachs Research Fund, University of Toronto.

REFERENCES

[1] T. Nicola, C. Leandro, C. Guido, and S. Enrico, "Masonry infilled frame structures: State-of-the-art review of numerical modelling," *Earthq. Struct.*, vol. 8, no. 1, pp. 225–251, 2015.

[2] S. C. Alih and M. Vafaei, "Performance of reinforced concrete buildings and wooden structures during the 2015 Mw 6.0 Sabah earthquake in Malaysia," *Eng. Fail. Anal.*, vol. 102, pp. 351–368, Aug. 2019.

[3] A. Menhrabi and P. Shing, "Performance of masonry - infilled R/C frames under in plane lateral loads : Analytical modeling," *Tech. Rep.*, vol. NCEER 94-0, pp. 45–50, 1994.

[4] F. Colangelo, "Pseudo-dynamic seismic response of reinforced concrete frames infilled with non-structural brick masonry," *Earthq. Eng. Struct. Dyn.*, vol. 34, no. 10, pp. 1219–1241, Aug. 2005.

[5] X. Gao, A. Stavridis, V. Bolis, and M. Preti, "Experimental study on the seismic performance of non-ductile RC frames infilled with sliding subpanels," *11th Natl. Conf. Earthq. Eng. 2018, NCEE 2018 Integr. Sci. Eng. Policy*, vol. 6, no. July, pp. 3927–3937, 2018.

[6] S. H. Basha and H. B. Kaushik, "A novel macromodel for prediction of shear failure in columns of masonry infilled RC frames under earthquake loading," *Bull. Earthq. Eng.*, vol. 17, no. 4, pp. 2219–2244, 2019.

[7] F. J. Vecchio and M. P. Collins, "The Modified Compression-Field Theory for Reinforced Concrete Elements Subjected to Shear," *ACI J.*, vol. 83, no. 2, pp. 219–231, Mar. 1986.

[8] F. J. Vecchio and M. P. Collins, "Response of Reinforced Concrete to In-Plane Shear and Normal Stresses," *Univ. Toronto. Dep. Civ. Eng.*, pp. 211–225, 1982.

[9] R. Park, M. J. N. Priestley, and W. D. Gill, "Ductility of square-confined concrete columns," *J. Struct. Div.*, vol. 108, no. ST4, pp. 929–950, 1982.

[10] E. C. Bentz, "Explaining the riddle of tension stiffening models for shear panel experiments," *J. Struct. Eng.*, vol. 131, no. 9, pp. 1422–1425, Sep. 2005.

[11] A. Brodsky, "A micro – macro modelling methodology for the analysis of infilled frames," *Bull. Earthq. Eng.*, vol. 19, no. 0123456789, pp. 2161–2184, Mar. 2021.

[12] D. Markulak, T. Dokšanović, I. Radić, and J. Zovkić, "Behaviour of steel frames infilled with environmentally and structurally favourable masonry units," *Eng. Struct.*, vol. 204, no. April 2019, 2020.

[13] P. S. Wong, F. J. Vecchio, and H. Trommels, "VECTOR2 & FORMWORKS USER'S MANUAL SECOND EDITION," 2013.